Journal of Renewable Materials

Tech Science Press

DOI: 10.32604/jrm.2023.026908

ARTICLE

Co-Production of High-Grade Dissolving Pulp, Furfural, and Lignin from Eucalyptus via Extremely Low Acid Pretreatment and Pulping Technologies and Catalysis

Chengxiang Li, Yue Wu, Chunhui Zhang*, Yao Liu, Qixuan Lin and Junli Ren*

State Key Laboratory of Pulp and Paper Engineering, School of Light Industry and Engineering, South China University of Technology, Guangzhou, 510640, China

*Corresponding Authors: Chunhui Zhang. Email: chunhui@scut.edu.cn; Junli Ren. Email: renjunli@scut.edu.cn

Received: 02 October 2022 Accepted: 27 October 2022

ABSTRACT

Hemicellulose and lignin are not reasonably utilized during the dissolved pulp preparation process. This work aimed to propose a process for the co-production of dissolving pulp, furfural, and lignin from eucalyptus. High-grade dissolving pulp was prepared from eucalyptus using a combination of extremely low acid (ELA) pretreatment, Kraft cooking, and elementary chlorine-free (ECF) bleaching. The obtained pre-hydrolysate was catalytic conversion into furfural in a biphasic system, and lignin during Kraft cooking and ECF was recovered. The process condition was discussed as well as the mass flow direction. The results showed that ELA pretreatment could effectively remove 80.1% hemicellulose. Compared with traditional hydrothermal pretreatment, the ELA pretreatment significantly increased the xylose yield from 5.05 to 14.18 g/L at 170°C for 2 h, which had practical significance for furfural production. The 82.7% furfural yield and 82.9% furfural selectivity were obtained from xylose-rich pre-hydrolysate using NaCl as a phase modifier in a biphasic system with 4-methyl-2-pentanone (MIBK) as an organic phase by ion exchange resin catalysts at 190°C for 2 h. Subsequently, the pretreated eucalyptus was subjected to Kraft cooking, and the optimal alkali amount was 14%. Then, the Kraft pulp was bleached using the O-D_1-E_P-D_2 sequence, and dissolving pulp was obtained with an ISO brightness of 86.0%, viscosity of 463 mL/g, and α-cellulose content of 95.4%. The Kraft lignin which has a potential application was investigated by 2D-HSQC NMR and ^{31}P NMR. The results showed that the S/G ratio of Kraft lignin was 1.93, and the content of phenolic hydroxyl groups was 2.53 mmol/g. Moreover, based on the above proposed process, 30.5 g dissolving pulp, 5.5 g furfural, and 21.2 g lignin per 100 g eucalyptus chips (oven dry) were produced. This research will provide new catalysis and pulping technical routes for dissolving pulp, furfural, and Kraft lignin products, which are in great demand in the chemical industry.

KEYWORDS

Eucalyptus; extremely low acid pretreatment; dissolving pulp; furfural; kraft lignin

1 Introduction

Owing to population growth, life quality improvement and fast-fashion trend, the demand for fiber in the textile market has increased significantly [1,2]. At present, synthetic fibers dominate the textile market, but the demand for cellulosic fiber is increasing in textile applications due to unique absorbency and moisture

management. Cellulosic fiber consumption is expected to increase from 3.7 kg per head today to 5.4 kg per head by 2030 [3]. Cotton linters and dissolving pulp are the major sources of regenerated cellulosic fibers, and the former is an ideal source. However, the growth of cotton requires specific climatic conditions, sufficient land, an excessive amount of water, and the use of pesticides, which have negative ecological and social consequences [4]. Therefore, it is difficult to achieve substantial growth in cotton production. Dissolving pulp is the most suitable substitute for cotton linters and has a broad market prospect. According to the statistical database released by the United Nations FAO shows, the global production of dissolving pulp increased from 3.42 million tons to 8.37 million tons between 2008 and 2018. During this period, the global dissolving pulp production increased by about 9% per year. If the production of dissolving pulp continues this growth pattern, the annual production of dissolving pulp will exceed 25 million tons after 2030 [5].

Dissolving pulp (DP) is a special chemical pulp with a high degree of purity α-cellulose (>90%) and a low content of hemicellulose (<5%), lignin (<0.1%), and resin [6,7]. At present, the commercial dissolving pulp production process mainly includes acid sulfite (AS) and pre-hydrolysis Kraft (PHK), and most dissolving pulp production lines use the latter [8]. Problems still exist in the production process of dissolving pulp, such as high production costs, product quality to be improved, and low utilization rate of hemicellulose and lignin [7]. Therefore, it is essential to improve the PHK process to improve the quality of dissolving pulp and reduce production costs.

The PHK process mainly includes the pre-hydrolysis, Kraft cooking, and bleaching stages. During the pre-hydrolysis stage, part of the hemicellulose in the biomass can be dissolved in the form of xylo-oligosaccharides and xylose, producing a large amount of xylose-rich pre-hydrolysate (PHL). The conventional treatment method of the factory is to concentrate the PHL, and send it to the alkali recovery furnace together with the black liquor produced in the cooking stage for combustion to recover energy. However, due to the small calorific value of hemicellulose, it is not cost-effective to recover energy through combustion, resulting in a serious waste of resources [9]. The pre-hydrolysate is rich in pentose sugars, which can be converted into valuable products like furfural [10]. Compared with recovering energy through combustion, catalytic conversion of xylose-rich pre-hydrolysate to furfural is more valuable. Furfural is an important feedstock in the chemical industry with a global market of about 300000 tons per year, and is listed as one of the top 12 value-added products by the U.S. Department of Energy (DOE) [11]. Therefore, catalytic conversion of xylose-rich pre-hydrolysate to furfural during the dissolving pulp production can give the industry additional economic benefits, and also provides a feasible scheme for the transition of dissolved pulp plants to integrated forest biorefineries [12]. Lignin is a by-product of the pulp and paper industry, with an annual output of about 50 million tons. However, only 2% of industrial lignin is used to produce valuable products [13]. Among all types of industrial lignin, Kraft lignin (KL) production is growing faster, which can be used as dispersants, bioplastics, carbon materials, etc. [14]. This makes it of great interest to understand the structural features for this type of lignin in order to assist in the commercial utilization of Kraft lignin.

Hemicellulose accounting for 20%–30% lignocellulose, is present as the depolymerization product during PHL, and increasing xylose yield in the pretreatment process can facilitate yielding more furfural during the dehydration. So we should strengthen the pretreatment process to improve the dissolution rate of xylose. In addition, it will inevitably increase the loss of cellulose and reduce the yield of dissolved pulp. Therefore, we should choose a relatively mild pretreatment technology. Extremely low acid (ELA) hydrolysis technology was first developed by U.S. National Renewable Energy Laboratory (NREL) for cellulose hydrolysis [15]. Low acid concentration (≤0.1 wt.%) and high temperature (160°C–220°C) are typical conditions for ELA pretreatment. The ELA technology has distinct advantages in biomass pretreatment. One is that the corrosion characteristics are very close to neutral water reaction, which can reduce equipment cost and maintenance. The second is minimal impact on the environment, which can be

considered as an eco-friendly process [16,17]. Lee et al. pretreated Saccharina japonica with 0.06% (w/w) sulfuric acid at 170°C for 15 min to obtain a maximum glucan content of 29.09% (w/w) [18]. Lee et al. pretreated Laminaria japonica with 0.10% H_2SO_4 at 170°C for 20 min to obtain a glucose release of 0.7 g/L in the pre-hydrolysate and 32.36% glucan content in the solid phase [17]. Hemicellulose is easier to be hydrolyzed than cellulose, so we consider applying extremely low acid to hemicellulose hydrolysis. According to previous research, oxalic acid has a high selectivity for hemicellulose hydrolysis in biomass [19,20]. In this work, extremely low oxalic acid (0.1 wt.% oxalic acid) was employed as a pretreatment solution.

As one of the most valuable and widely planted hardwoods in the world, eucalyptus is an important feedstock of pulp because of its rapid growth and wide adaptability [21]. Eucalyptus contains high carbohydrate (cellulose and hemicellulose), which has enormous potential as raw materials for the production of valuable materials, such as dissolving pulp, furfural, and other industrial products [22]. Thus, eucalyptus was employed as raw material in this study. Herein, this work was to propose a new process for the co-production of dissolving pulp, furfural and lignin, and the specific process flow diagram was shown in Fig. 1. High-grade dissolving pulp was prepared from eucalyptus using a combination of extremely low acid (ELA) pretreatment, Kraft cooking, and elementary chlorine-free (ECF) bleaching. The xylose-rich pre-hydrolysate was converted into furfural by catalytic technology. During ELA pretreatment, most of the hemicellulose was removed, which could reduce the amount of alkali used in the alkali cooking process. Also, we could get Kraft lignin from the cooking process. This research will provide new catalysis and pulping technical routes for dissolving pulp, furfural, and Kraft lignin products, which are in great demand in the chemical industry.

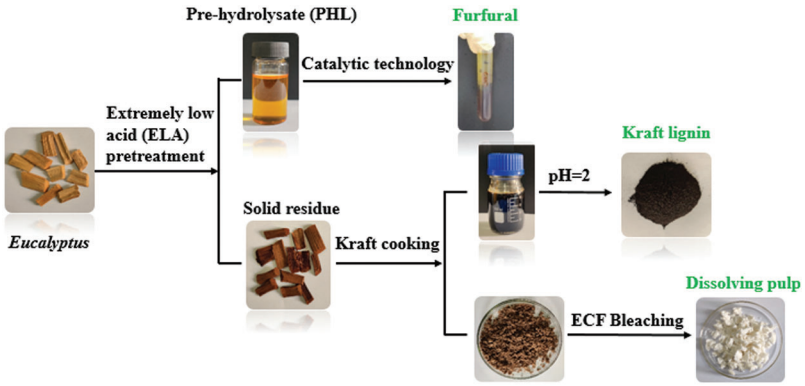

Figure 1: The process flow diagram of co-production of dissolving pulp, furfural, and kraft lignin

2 Materials and Methods

2.1 Materials

Oxalic acid (AR, 98%), NaOH (AR, 96%), $Na_2S{\cdot}9H_2O$ (AR, ≥98.0%), H_2O_2 (AR, 30 wt.% in H_2O), Toluene (≥99.5%), ion exchange resin (CAS number: 9037-24-5) and $MgSO_4$ (AR) were purchased from Aladdin China. ClO_2 (Available chlorine content: ≥8.0%) were purchased from Xiya Reagent (Shan dong, China). 4-Methyl-2-pentanone (MIBK, AR, 99.0%) and 2-Methyltetrahydrofuran (2-Me-THF, 99%) were purchased from Macklin Reagent Co., Ltd., Shanghai, China. Eucalyptus (*Eucalyptus Grandis.*) chips were obtained from a forest farm in Guangxi Province (China), and it was chipped to a size of 20 mm × 15 mm × 2–3 mm. Samples of the untreated and pretreated eucalyptus chips were ground using a biomass pulverizer. The fraction passing between 40 and 60 mesh of ground wood powder was collected for chemical analysis. The chemical composition of eucalyptus was determined according to the standard laboratory analytical procedure developed by the National Renewable Energy Laboratory (NREL) [23].

The eucalyptus was composed of 0.9% benzyl-ethanol extractives, 44.3% glucan, 15.9% xylan, 31.1% lignin (27.3% acid-insoluble lignin and 3.8% acid-soluble lignin) and 8.7% others.

2.2 Extremely Low Acid (ELA) Pretreatment

The eucalyptus chips and extremely low acid (ELA, 0.1 wt.% oxalic acid solution) were added to a reaction kettle with lining Teflon at a solid-to-liquor ratio of 1:8 (g/mL). The mixture was heated to reach the desired maximal temperature (160°C~190°C) in a high temperature drying oven and was held for a certain time (1.0~3.0 h). After the reaction, the reaction kettle was cooled in a cold water bath. Subsequently, the solid residual fractions and liquid fractions (pre-hydrolysate, PHL) were separated with a crucible filter G3. The products in the liquid fractions were determined by high-performance liquid chromatography (HPLC). The solid residual fractions were thoroughly washed until neutral with deionized water and then oven-dried at 105°C for solid yield determination. The pH of the mixture before and after the extremely low acid pretreatment was recorded. The traditional hydrothermal pretreatment was used as the blank group.

2.3 Kraft Cooking

Kraft cooking of the solid residual fractions under optimum pretreatment conditions was carried out in a rocking-type digester with six one-liter vessels (Green Wood 2201-6, USA). The cooking liquor contained NaOH and Na_2S, and the solid-to-liquid ratio was 1:5 (g/mL). The amount of effective alkali (calculated as Na_2O) on eucalyptus chips (oven dry) ranged from 12% to 16% and the sulfidity (calculated as Na_2O) was 25%. The maximum cooking temperature was 160°C. The heating time from room temperature to maximum temperature was 90 min and then was held for 30 or 60 min.

After Kraft cooking, the pulp was washed thoroughly to neutral with deionized water. Then the pulp was screened using a vibrating flat screen (Messmer Somerville, Germany) equipped with a 0.2-mm-wide slotted plate. The screened pulps were put in polyethylene bags and stored at 4°C for further bleaching. The pulp yield was determined by the gravimetric method. Kraft lignin (KL) was obtained by adjusting the pH of the black liquor to pH 2 with H_2SO_4. Milled wood lignin (MWL) was prepared according to Bjorkman's method [24].

2.4 Bleaching

The Kraft pulp under optimum cooking conditions was subjected to ECF bleaching using the O-D_1-E_P-D_2 sequence, and the bleaching conditions of each stage were shown in Table 1. The O stage was carried out using a 1L high pressure reactor (PARR, America). The Kraft pulp and bleaching liquor were mixed in a polyethylene bag, and the bag was placed in a water bath for D_1, E_p, and D_2 stages. The pulp was thoroughly washed to neutral after each stage. The dissolved pulp was obtained after ECF bleaching. Ultimately, the dissolving pulp yield was determined by the gravimetric method.

2.5 Furfural Production

Catalytic conversion of xylose-rich pre-hydrolysate to furfural was conducted according to the method of our research groups [25,26]. The pre-hydrolysate was carried out in a reaction kettle. A certain amount of catalyst (ion exchange resin) and NaCl were added to the reaction kettle. And then pre-hydrolysate (aqueous phase) and organic solvents (organic phase) were poured into the above reactor to form a biphase system at a ratio of 1:1 (v/v). The reactor was put in a heat-collecting magnetic stirrer (DF-101S, China) and heated at 190°C for 2 h. After the reaction, the reaction solution was cooled and filtered with 0.22 μm syringe filter prior for HPLC analysis.

Table 1: Bleaching conditions of O-D_1-E_P-D_2 sequence

Stage	O	D_1	E_P	D_2
Temperature (°C)	90	70	70	70
Reaction time (min)	60	60	60	60
Pulp consistency (%)	10	10	10	10
NaOH dosage (%)	3	-	2	-
$MgSO_4$ dosage (%)	0.6	-	0.5	-
Oxygen pressure (Psi)	100	-	-	-
ClO_2 dosage (%)	-	1.2	-	0.5
H_2O_2 dosage (%)	-	-	0.5	-
Final pH	11.5	2.5	11.4	4.2

Note: O: oxygen, D: dioxide chlorine, P: peroxide hydrogen, E: alkali extraction.

2.6 Characterization of Solid Residue

The solid residue samples were ground into powder. The chemical composition of solid residue fraction was also determined by the NREL method. Cellulose recovery, xylan removal, and lignin removal were calculated according to the following equations:

$$\text{Cellulose recovery } (\%) = \frac{\text{Glucose in solid residue (g)}}{\text{Glucose in raw material (g)}} \times 100\% \quad (1)$$

$$\text{Xylan removal } (\%) = 1 - \frac{\text{Xylose in solid residue (g)}}{\text{Xylose in raw material (g)}} \times 100\% \quad (2)$$

$$\text{Lignin removal } (\%) = 1 - \frac{\text{Lignin in solid residue (g)}}{\text{Lignin in raw material (g)}} \times 100\% \quad (3)$$

For FT-IR analysis, the untreated and pretreated powder samples were mixed with KBr and pressed into thin pellets. Then the thin pellets were scanned with a Fourier Transform infrared (FT-IR) spectrometer (Nicolet IS50, Thermo Fisher Scientific, USA), recorded from 4000 to 400 cm^{-1} at a resolution of 4 cm^{-1}.

For XRD analysis, the untreated and pretreated powder samples were analyzed by an X-ray diffractometer (XRD) (SmartLab 9 kW, Rigaku, Japan). The scattering angle (2θ) ranged from 10° to 40° with a step size of 0.04°. The crystallinity index (CrI) was calculated according to the following equations determined by Segal et al. [27]:

$$\text{CrI} = (I_{002} - I_{am})/I_{002} \times 100\% \quad (4)$$

where I_{002} was the intensity of the crystalline peak at about $2\theta = 22.6°$, attributed to crystalline regions, and I_{am} was the intensity at about $2\theta = 18.5°$, attributed to amorphous regions.

Thermogravimetric analysis (TGA) of the untreated and pretreated solid residues was carried out on a Netzsch TG209F3 (Germany) instrument. Samples of about 10 mg were heated in a temperature range from 40°C to 700°C at a heating rate of 10 °C/min under nitrogen atmosphere.

Scanning electron microscopy (SEM) images of the untreated and pretreated eucalyptus samples were carried out using a Hitachi SU5000 (Japan) instrument at 5 kV acceleration voltages.

2.7 Determination of Pulp Properties

The α-cellulose content of the pulps was determined according to TAPPI T203 om-09. The viscosity was measured according to TAPPI T230 om-08. The Kappa number was determined according to TAPPI T236 cm-85. The brightness test was carried out using a brightness meter (Elrepho 070, L&W, Sweden) according to TAPPI T452 om-08.

2.8 Characterization of Lignin

The structure of lignin samples was analyzed by ^{1}H–^{13}C heteronuclear singular quantum correlation (HSQC) nuclear magnetic resonance (NMR) (600 MHz, Bruker, Germany). Specific parameters are as follows: H(0∼10)ppm, D1 = 1.5 s, Td = 1024; C(0∼170)ppm, TD = 256, NS = 64.

The content of the hydroxyl group in lignin samples was determined by quantitative ^{31}P NMR. ^{31}P NMR spectra were recorded on a spectrometer (400 MHz, Bruker, Germany).

2.9 Analysis of Pre-Hydrolysate before and after Catalysis

The glucose, xylose, formic acid, acetic acid, 5-hydroxymethylfurfural (HMF) and furfural concentrations were determined by HPLC (Agilent, 1260 Infinity II, USA) equipped with a refractive index detector. The sample separation was performed using an HPX-87H (BIO-RAD) at 60°C, and the mobile phase used was 5 mmol sulfuric acid at a flow rate of 0.5 mL/min. Furfural yield, xylose conversion, and furfural selectivity were calculated according to the following equations:

$$\text{Furfural yield (mol \%)} = \frac{\text{Mole of furfural produced}}{\text{Mole of xylose in pre} - \text{hydrolysate}} \times 100\% \quad (5)$$

$$\text{Furfural selectivity (mol \%)} = \frac{\text{Mole of furfural produced}}{\text{Mole of xylose reacted}} \times 100\% \quad (6)$$

$$\text{Xylose conversion (mol \%)} = \frac{\text{Mole of xylose reacted}}{\text{Mole of xylose in pre} - \text{hydrolysate}} \times 100\% \quad (7)$$

3 Results and Discussion

3.1 Effects of Pretreatment Conditions on Xylose Yields

Xylose is the main component of the pre-hydrolysate and is used as the raw material for the production of furfural. In order to increase the furfural production, we need to increase the xylose yield in the pre-hydrolysate. Therefore, we added extremely low acid to assist the traditional hydrothermal pretreatment to improve the xylan dissolution rate and xylose yield. We compared the effects of conventional hydrothermal pretreatment and extremely low acid pretreatment on xylose yields.

Fig. 2 showed the time profiles of xylose concentration in pre-hydrolysate at different temperatures. For hydrothermal pretreatment (Fig. 2A), the xylose concentration increased with time during the initial stage of hydrolysis for all temperatures. However, the xylose concentration reduced after reaching a maximum for temperatures higher than 170°C, and this inflection point came earlier with increasing temperature. This result was attributed to the fact that the rate of xylose dissolution was lower than that of xylose degradation to furfural [28]. In comparison to hydrothermal pretreatment, importantly, the addition of extremely low acid significantly increased the xylose concentration from 5.05 g/L (25.4% xylose yield) to 14.18 g/L (71.3% xylose yield) at 170°C for 2 h. Although the xylose concentration at 170°C for 2 h is not the highest but acceptable, higher temperature will inevitably lead to the loss of more glucose, which is not conducive to the yield of dissolving pulp.

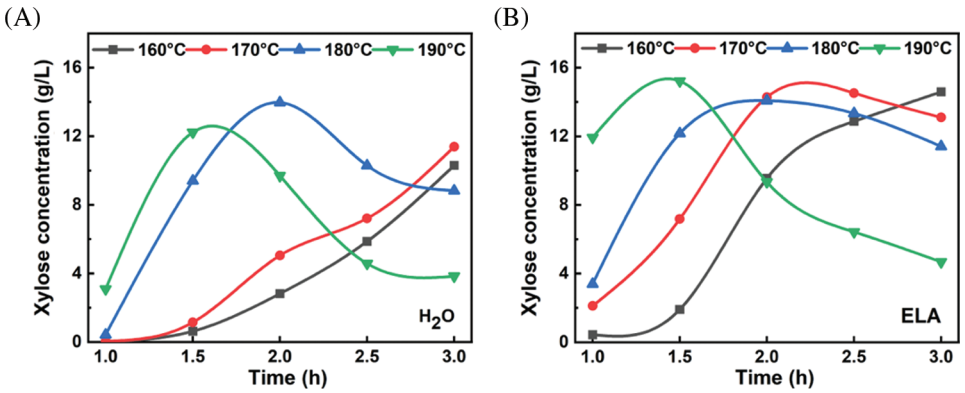

Figure 2: The time profiles of xylose concentration in pre-hydrolysate at different temperatures by (A) hydrothermal pretreatment and (B) extremely low acid pretreatment

To verify the advantage of extremely low acid in pretreatment, we determined the carbohydrate and lignin content of solid residues under several specific conditions (170°C-2 h-ELA, 170°C-2 h-H_2O, and 180°C-2 h-H_2O were investigated) by the NREL method. As shown in Table 2, the addition of extremely low acid significantly increased the xylose removal from 45.5% to 80.1% under the same pretreatment condition (170°C, 2 h), which was consistent with the xylose concentration in the pre-hydrolysate. In addition, 170°C-2 h-ELA was better than 180°C-2 h-H_2O in terms of cellulose retention and xylan removal rate. Therefore, under the condition of achieving the same pretreatment effect, adding a trace amount of oxalic acid can lower the reaction temperature by 10°C, and simultaneously improve the xylose yield significantly. This strategy of extremely low acid pretreatment is significant for energy saving. Interestingly, the lignin removal rate of 170°C-2 h-H_2O was higher than that of 170°C-2 h-ELA, which was attributed to the formation of a lignin-like material termed pseudo-lignin during pretreatment [29].

Table 2: The carbohydrate and lignin content of solid residues under several specific conditions

Conditions	Yield, %	Glc, %	Xyl, %	AIL, %	ASL, %	Total lignin, %	Cellulose recovery, %	Xylan removal, %	Lignin removal, %
Untreated	100	44.3	15.9	27.3	3.8	31.1	-	-	-
170°C-2 h-ELA	75.5	56.4	4.2	33.8	2.2	36.0	96.1	80.1	12.6
170°C-2 h-H_2O	80.2	53.5	10.8	30.3	2.4	32.7	96.9	45.5	15.7
180°C-2 h-H_2O	75.4	55.5	5.3	33.5	1.9	35.4	94.7	74.9	14.2

Note: glucan (Glc), xylan (Xyl), acid insoluble lignin (AIL), acid soluble lignin (ASL); Total lignin % = acid insoluble lignin (AIL %) + acid soluble lignin (ASL %).

3.2 Effects of Extremely Low Acid Pretreatment on Composition of Eucalyptus

Compositional analysis was performed on the untreated and pretreated eucalyptus samples in order to understand the effects of extremely low acid pretreatment on its chemical composition, and the results were shown in Fig. 3. As expected, the solid yield decreased with increasing temperature and prolonged time, which was attributed to the dissolution of the main components in biomass [30]. For example, the solid yield declined from 80.6% to 70.2% with the pretreatment temperature increasing from 160°C to 190°C (2 h), and the solid yield declined from 91.7% to 71.8% with the pretreatment time increasing from 1.0 to 3.0 h (170°C).

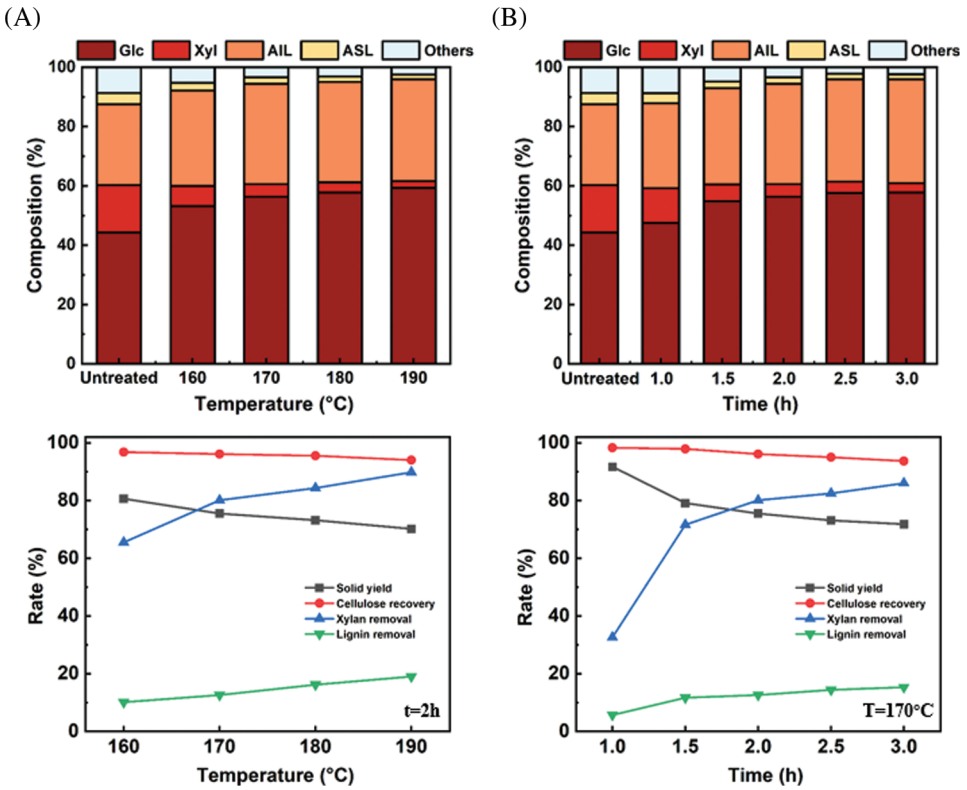

Figure 3: Variation of chemical components, solid yield, cellulose recovery, xylan removal and lignin removal rate before and after extremely low acid pretreatment

As shown, the content of glucan and xylan changed obviously after the extremely low acid pretreatment. The glucan content increased from 44.3% in the untreated eucalyptus to 56.4% at 170°C for 2 h. Meanwhile, the xylan content decreased significantly from 15.9% in the untreated eucalyptus to 4.2% at 170°C for 2 h. Compared with the changes in glucan and xylan contents, the total lignin showed a relatively small change after the pretreatment. The calculated lignin removal rate was 10.1% at (160°C, 2 h) and it increased to 19.0% (190°C, 2 h). Whereas for xylan, the removal rate increased from 65.5% (160°C, 2 h) to 89.8% (190°C, 2 h). The contents of glucan, xylan, and lignin were gradually stabilizing after 2 h at 170°C. Overall, extremely low acid pretreatment can remove hemicellulose effectively, and has little effect on cellulose.

3.3 Chemical Composition Analysis of Pre-Hydrolysate

The effects of pretreatment time and temperature on the compositions of the pre-hydrolysate were shown in Table 3. The pH values of the pre-hydrolysate increased from 2.13 to 2.77 at 170°C, mainly due to the interaction result of hemicellulose acid hydrolysis and the exchange reaction of H^+ with inorganic ions in the wood [31]. This phenomenon was consistent with the results reported by Lin et al. [32]. The yield of glucose increased from 0.54 to 1.81 g/L with the increase of the pretreatment temperature from 160°C to 190°C at the same time of 2 h. The glucose content in the pre-hydrolysate was much lower than that of xylose, indicating that the release and depolymerization of hemicellulose from lignocellulosic biomass were much easier than cellulose [33]. Moreover, under acidic conditions during the pretreatment process, the hexose mono sugars underwent sugar dehydration reactions to form HMF, and the pentose mono sugars underwent sugar dehydration reactions to form furfural. The furfural yield increased slowly from

0 to 0.29 g/L before 1.5 h at 170°C, and the furfural yield significantly increased to 4.12 g/L at 190°C for 2 h. This indicated that a higher temperature and longer time can accelerate the dehydration of xylose into furfural. The content of HMF was not detected before 1.0 h at 170°C, and the content increased slowly as the reaction proceeded, compared with the furfural content. The reason is that the conversion of glucose into HMF is more difficult than the conversion of xylose into furfural under this condition, and the content of glucose is much lower than that of xylose [34]. Formic acid was generated by the degradation of HMF and furfural, and acetic acid was generated by hydrolyzing acetyl groups. The yields of formic acid and acetic acid were 1.13 and 7.63 g/L, respectively, at 170°C for 2 h.

Table 3: Chemical composition of pre-hydrolysate

Entry	Condition T-t (°C-h)	pH	Glucose (g/L)	Xylose (g/L)	FA (g/L)	AA (g/L)	HMF (g/L)	FF (g/L)
1	170–1.0	2.36	0.22	2.12	0.23	1.23	ND	<0.01
2	170–1.5	2.39	0.61	7.18	0.94	4.49	0.04	0.29
3	170–2.0	2.52	0.95	14.18	1.13	7.63	0.09	0.93
4	170–2.5	2.66	1.29	14.62	0.80	8.16	0.16	1.56
5	170–3.0	2.77	1.26	13.10	0.66	8.92	0.25	2.65
6	160–2.0	2.39	0.54	10.08	0.92	5.02	0.01	0.27
7	180–2.0	2.75	1.28	13.96	0.72	8.17	0.22	1.92
8	190–2.0	2.92	1.81	9.70	0.77	8.97	0.68	4.12

Note: FA: formic acid, AA: acetic acid, HMF: 5-Hydroxymethylfurfural, FF: furfural; ND: not detectable; Initial pH: 2.13.

3.4 Characterization of Solid Residue

3.4.1 FT-IR Analysis

In order to compare the structural changes of eucalyptus, the FT-IR spectra of eucalyptus and pretreated solid residues under extremely low acid pretreatment were illustrated in Fig. 4. For the untreated eucalyptus raw material, two distinct peaks at 1735 and 1234 cm^{-1} are ascribed to C=O and C-O stretching vibrations of the acetyl ester in hemicelluloses, respectively [22]. However, the intensity of the two peaks became weaker with the intensification of pretreatment conditions (increasing reaction temperature or reaction time). Even the C=O bond at 1735 cm^{-1} disappeared at 170°C for 3 h. This indicated that the acetyl group of hemicellulose was basically completely removed during pretreatment. In addition, the peaks at 1160 and 898 cm^{-1} are ascribed to C-O-C vibrations and C-O-C stretching at β-glucosidic linkages in carbohydrates, respectively. Under the condition that the reaction temperature was lower than 170°C and the reaction time was less than 2 h, the intensity of these two peaks was not significantly weakened. This indicated that part of the cellulose was degraded during the extremely low acid pretreatment, but the amount of cellulose degradation was acceptable. Moreover, the peak intensity around 1600, 1510, 1459, and 1427 cm^{-1} in all spectra of pretreated eucalyptus was higher than of untreated eucalyptus, indicating pretreated solid residues had higher lignin contents [35]. These results can be verified by the lignin content in Table 2.

3.4.2 XRD Analysis

X-ray diffraction (XRD) patterns can be used to analyze the changes in crystallinity and crystal structure of cellulose during pretreatment. The XRD patterns and calculated crystallinity index (CrI) of untreated eucalyptus and pretreated solid residues under extremely low acid pretreatment were shown in Fig. 5. In all samples, two typical diffraction peaks were detected 2θ at approximately 15.5° and 22.6°, which were

assigned to the 101 peak (I_{101}) and the 002 peak (I_{002}) in cellulose I, respectively [36]. This indicated that extremely low acid pretreatment did not change the crystal structure of cellulose. Under a specific time (2.0 h), the CrI of pretreated solid residues increased from 53.6% at 160°C to 65.8% at 190°C with the increase in pretreatment temperature. Under a specific temperature (170°C), the CrI of pretreated solid residues increased from 45.7% in 1.0 h to 65.6% in 3.0 h with the prolongation of pretreatment time. The CrI of pretreated solid residues ranged from 45.7%–65.8%, which was higher than that of untreated eucalyptus raw materials (42.8%). The increase of cellulose CrI was ascribed to the removal of most amorphous hemicellulose during the pretreatments, which increased the relative content of cellulose, as well as the amorphous region of part of the cellulose, was destructed [22].

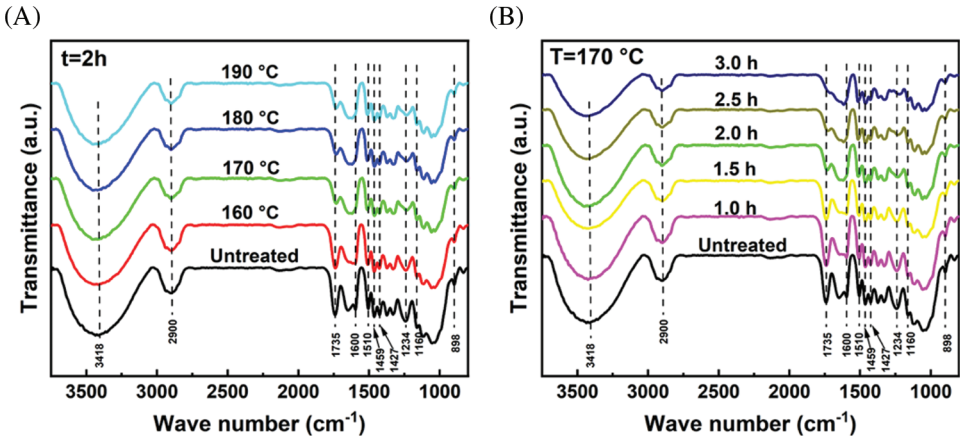

Figure 4: FT-IR spectra of eucalyptus before and after extremely low acid pretreatment with different conditions

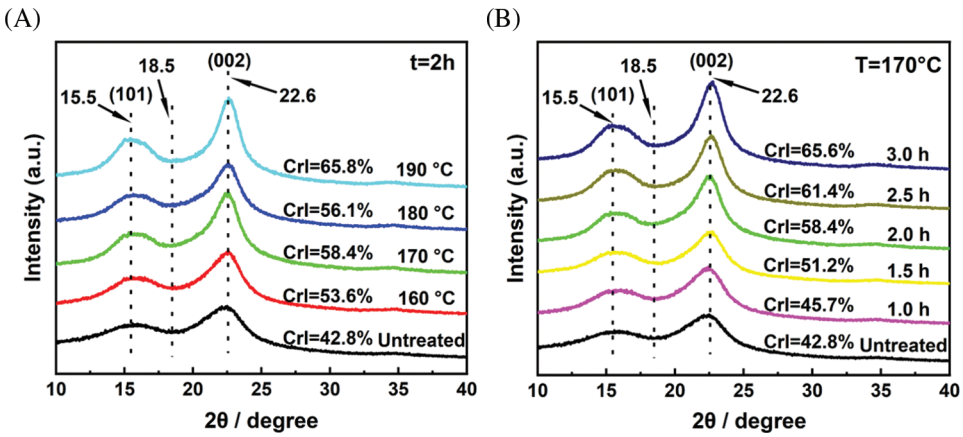

Figure 5: XRD patterns of eucalyptus before and after extremely low acid pretreatment with different conditions

3.4.3 SEM Analysis

The morphological structures of untreated and pretreated eucalyptus samples were illustrated in Fig. 6. The color of the eucalyptus changed from yellow to dark brown after extremely low acid pretreatment, and became darker as the pretreatment conditions became severe. The untreated eucalyptus sample exhibited a

smooth and compact surface structure in the SEM images. However, the surface of solid residue became rough after pretreatment, and a large number of holes and fragments of various sizes can be observed, caused by the dissolution of hemicelluloses from the cell wall of eucalyptus [33]. As expected, at a higher pretreatment temperature or a longer pretreatment time, the originally smooth structure was more severely destroyed, and more obvious cracks appeared, such as 190°C–2.0 h. Interestingly, many spherical droplets on the fiber surface were observed clearly. There are reports that when the pretreatment temperature reaches above the lignin phase transition range (140°C), lignin will coalesce into larger molten bodies that move inside and outside the cell wall, and can redeposit on the surface to form spherical droplets when encountering water [35,37]. This phenomenon was consistent with the results reported by Xiao et al. [38].

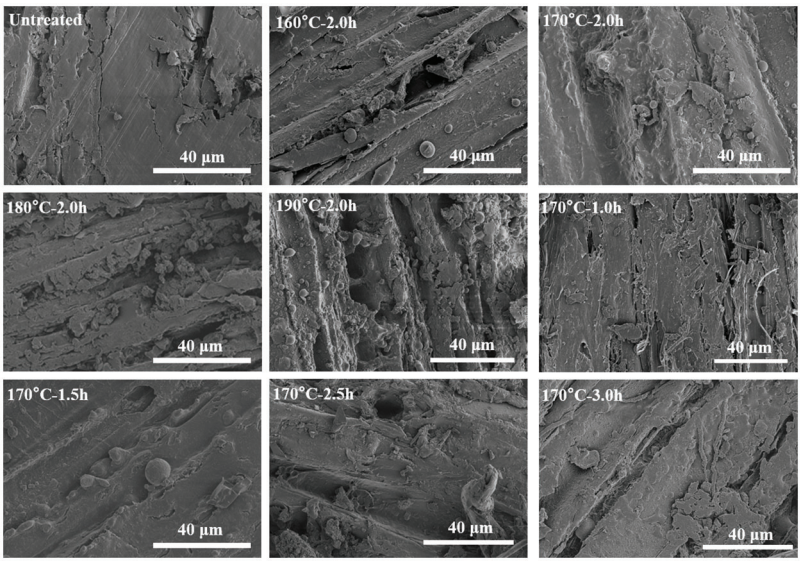

Figure 6: SEM images of eucalyptus before and after extremely low acid pretreatment with different conditions

3.4.4 Thermal Analysis

Thermogravimetric analysis (TGA) and first derivative thermogravimetric (DTG) curves were used to analyze the changes in the thermal properties of materials before and after extremely low acid pretreatment. As shown in Fig. 7A, the curves can be mainly divided into two stages. The first stage was the rapid weight loss stage that occurred around 240°C to 360°C, which was attributed to the degradation of carbohydrates (cellulose and hemicellulose). The second stage was the slow weight loss stage that occurs around 360°C to 600°C, which was attributed to the degradation of lignin. It is clearly shown from the DTA curves (Fig. 7B) that the peak at 240°C–300°C for sample b and sample c disappeared compared to untreated sample a, which was attributed to the efficient removal of hemicellulose during pretreatment [38]. In addition, the weight loss rate of sample c was less than that of sample b, which also indicated that the addition of extremely low acid can improve the removal rate of hemicellulose.

3.5 Optimization of Kraft Pulping Conditions

After extremely low acid pretreatment, the solid residues were subjected to Kraft cooking for removing lignin and fractionating cellulose from pretreated solid residue. As a measure of cooking efficiency during Kraft cooking, the degree of delignification is considered a significant parameter. Kraft pulp is evaluated for cooking efficiency based on the Kappa number, which represents the residual lignin content.

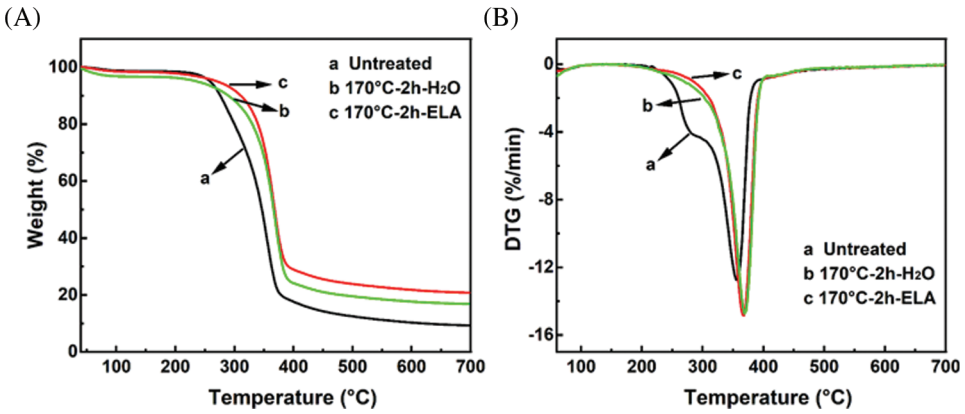

Figure 7: (A) TGA and (B) DTG distributions of the untreated and pretreated eucalyptus

The effects of alkali charge and soaking time on the properties of Kraft pulps were shown in Table 4. As shown, increasing the alkali charge under constant soaking time or increasing the soaking time under constant alkali charge resulted in a significant decrease in Kappa number and viscosity. For example, under a specific soaking time (30 min), the pulp Kappa number and viscosity at an alkali charge of 14% were 18.8 and 927 mg/L, respectively; whereas the Kappa number and viscosity at an alkali charge of 16% were reduced to 16.7 and 852 mg/L, respectively. The pulp yield at an alkali charge of 12% was lower than that of an alkali charge of 14%, due to the fact that the low residual alkali concentration (0.8 g/L) caused the cooking liquor not to permeate into the solid residue, so that a small portion of the solid residue did not form pulp. When the alkali charge was ≥14%, the pulp yield was consistent with Kappa number and viscosity. The residual alkali of the black liquor after cooking should be controlled in the range of 6 g/L∼10 g/L [39]. Taking into account the severity of delignification and the pulp yield, the cooking conditions were determined as follows: alkali charge was 14%, and holding time was 30 min.

Table 4: Cooking conditions and results

Entry	Alkali charge %	Soaking time, min	Pulp yield, %	Kappa number	Residual alkali, g/L	Viscosity, mg/L
1	12	30	32.9	22.6	2.3	1074
2	14	30	34.1	18.8	6.0	927
3	16	30	33.4	16.7	9.4	852
4	12	60	33.2	20.5	0.8	1011
5	14	60	33.0	17.3	3.5	915
6	16	60	32.3	15.8	5.1	798
7	16	30	35.9	19.7	9.7	987

Note: 1–6: ELA, 7: H_2O.

Compared to eucalyptus treated with hydrothermal pretreatment (Entry 7), the addition of extremely low acid (Entry 2) can significantly reduce the alkali charge (by about 10%, from 16% to 14%) in the cooking stage, which was due to the removal of more hemicellulose in the pre-hydrolysis stage [40]. Moreover, in terms of kappa number and viscosity, the addition of extremely low acid is positive for cooking pulp; in terms of pulp yield, the addition of extremely low acid is negative but acceptable.

3.6 Evolvement of Pulp Properties During Bleaching

The bleaching sequence of O-D_1-E_P-D_2 is a typical elemental chlorine-free (ECF) bleaching technique [41]. During the O-D_1-E_P-D_2 bleaching process, the change of pulp properties (kappa number, brightness, viscosity, and α-cellulose) was studied, and the detailed results were shown in Fig. 8.

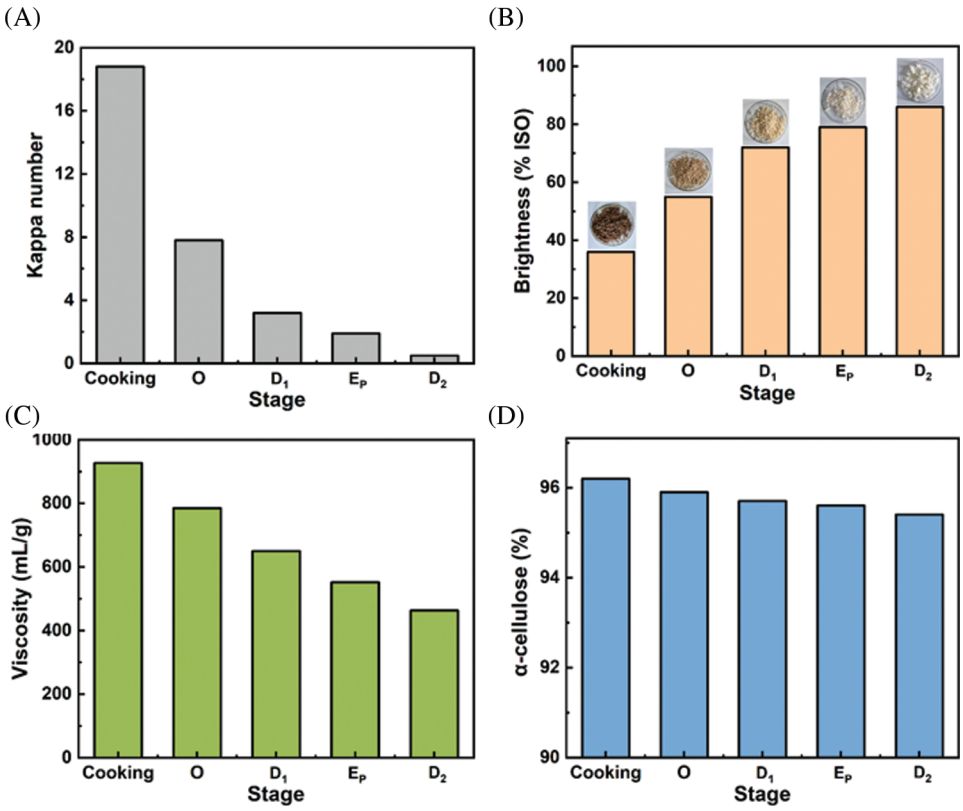

Figure 8: Changes of pulp properties during the O-D_1-E_P-D_2 bleaching process

As shown in Fig. 8A, the Kappa number of pulp decreased significantly from 18.8 to 7.8 in the O stage, indicating that the lignin in pulp was effectively removed, and it was the stage with the highest amount of delignification in the bleaching process. The residual lignin was further removed in the following D_1-E_P-D_2 stages, and the Kappa number of the final dissolving pulp product was 0.6, implying the lignin content in the final product was negligible. Moreover, we can obviously observe the brightness changes of pulp from the cooking stage to the D_2 stage (Fig. 8B). The pulp was bleached by the O-D_1-E_P-D_2 sequence to a target brightness of 82% ISO, and the dissolving pulp final brightness was 86% ISO. The viscosity of the pulp dropped gradually during the bleaching stage (Fig. 8C), which can be attributed to the chlorine dioxide used in the D1/D2 stage and the hydrogen peroxide used in the E_P stage [42]. The dissolving pulp's final viscosity was 463 mg/L. However, the decrease of viscosity did not result in a significant loss of α-cellulose content (Fig. 8D). Compared with the pulp in the cooking stage (α-cellulose of 96.2%), the α-cellulose content of the final dissolving product decreased only to 95.4%. To sum up, the Kraft pulp obtained after extremely low acid pretreatment and Kraft cooking was efficiently bleached through the O-D_1-E_P-D_2 bleaching sequence. High-grade eucalyptus dissolving pulp with ISO brightness of 86.0%, viscosity of 463 mL/g, and α-cellulose content of 95.4% was produced.

The properties of dissolving pulp obtained by different pretreatment methods were shown in Table 5. Compared with the traditional hydrothermal pretreatment (Entry 1), the dissolving pulp obtained by extremely low acid pretreatment and Kraft cooking and bleaching (Entry 2) had the desirable properties such as high α-cellulose content, high brightness, and low pentosane content, especially the cellulose content was increased from 92.9% to 95.4%, reaching the grade of excellent products in the light industry standard. In addition, extremely low acid pretreatment decreased the viscosity and degree of polymerization of the pulp and had a negligible effect on the properties of the dissolving pulp, which was attributed to the fact that the loss of a small part of cellulose during pretreatment.

Table 5: Properties of dissolving pulp

Entry	α-cellulose, %	Viscosity, mL/g	DP	Brightness, ISO	Pentosane, %	Ash
1	92.9	483	674	82	2.55	0.10
2	95.4	463	642	85	1.07	0.08
3	≥93.0	380–500	-	≥82	≤4.00	≤0.13

Note: 1: Hydrothermal pretreatment, 2: ELA pretreatment, 3: Industry standard for light industry; DP: degree of polymerization.

3.7 Furfural Production

As shown in Table 6, the furfural yield and the xylose conversion were 36.9% and 61.2%, respectively in pure water (Entry 2). Without the catalysts (entry 1), furfural yield up to 28.0%, because more acetic acid and other acids function. Compared with entry 1, the addition of catalyst (entry 2) can improve furfural yield and xylose conversion, but a modest increase was observed. To further improve the furfural yield, organic solvent as the organic phase was added to form a biphase system. The relatively high furfural yields were obtained in various biphasic systems (Entries 3–5), including PHL/Toluene (44.8%), PHL/2-Me-THF (48.0%), and PHL/MIBK (55.9%). This was attributed to the fact that furfural was quickly extracted into the organic phase after formation in a biphase system, and was related to the partition coefficients of furfural in biphasic systems (MIBK/H_2O > 2-Me-THF/H_2O > Toluene/H_2O) [43,44]. The furfural yield still did not reach the desired yield under the biphasic system (>80%). According to previous studies [25,44], adding sodium chloride to the biphasic system can change the intermolecular bonding interactions between liquid components, thereby promoting the extraction of furfural from the aqueous phase to the organic phase. Based on this, we considered adding sodium chloride into the biphasic system to further improve the furfural yield. As expected (Entry 6), the 82.7% furfural yield, 99.8% xylose conversion, and 82.9% furfural selectivity were obtained, which were significantly higher than those of the system without sodium chloride (Entry 5%, 55.9%, 66.0%, and 84.7%). So far, satisfactory results have been achieved.

Table 6: Results for the conversion of xylose-rich pre-hydrolysate to furfural with different conditions

Entry	Catalyst	NaCl, mg/ml	Organic phase	Furfural yield, %			Xylose conversion, %	Furfural selectivity, %
				Organic	Aqueous	Total		
1	-	0	None	ND	28.0	28.0	53.0	52.8
2	+	0	None	ND	36.9	36.9	61.2	60.3
3	+	0	Toluene	35.6	9.2	44.8	58.7	76.3
4	+	0	2-Me-THF	39.9	8.1	48.0	57.2	83.9
5	+	0	MIBK	48.0	7.9	55.9	66.0	84.7
6	+	160	MIBK	78.9	3.8	82.7	99.8	82.9

Note: Reaction conditions: 50 mg catalyst, 190°C, 2 h; the volume ratio of organic phase and aqueous phase was 1:1; "+" refers to the addition of the catalyst; "-" refers to the absence of the catalyst; ND: not detectable.

3.8 Recovered Kraft Lignin Structure

3.8.1 2D-HSQC NMR Analysis

The detailed structural information of MWL and KL can be obtained through 2D-HSQC NMR spectra. The distribution of lignin signals was referred to the published literature [45–47]. The assignment of $^{13}C–^{1}H$ cross-signals of lignin was shown in Table 7. In the NMR spectrum, the side-chain (δ_C/δ_H 50–90/2.5–6.0) and aromatic (δ_C/δ_H 100–135/5.0–8.0) regions of lignin were shown in Fig. 9. In the side-chain region of lignin, the methoxy groups (-OMe), β-aryl-ether (β-O-4, A), resinol (β-β, B) and phenylcoumaran (β-5, C) were observed. In the aromatic region of lignin, the signals of S-type and G-type units were observed, while the signals of H-type units were not detected. This suggested that the structural units of eucalyptus lignin were mainly S-type and G-type [48]. The NMR spectrum could obviously reflect the structural differences between MWL and KL. Compared with the MWL, it could be clearly observed that the β-5 structures' signals disappeared in the spectra of KL. This indicated that the β-5 linkages were cleaved during the Kraft cooking process. Moreover, part of S-type lignin was condensed at δ_C/δ_H 106.22/6.49.

Table 7: Assignment of $^{13}C–^{1}H$ cross-signals of lignin

Lable	δC/δH (ppm)	Assignment
C_β	53.1/3.46	C_β–H_β in phenylcoumaran substructures (C)
B_β	53.72/3.11	C_β–H_β in resinol substructures (B)
-OMe	56.27/3.75	C–H in methoxyls
A_γ	60.40/3.72	C_γ–H_γ in β-O-4 substructures (A)
C_γ	62.2/3.76	C_γ–H_γ in phenylcoumaran substructures (C)
B_γ	71.60/4.19 and 3.84	C_γ–H_γ in resinol substructures (B)
A_α	72.36/4.91	C_α–H_α in β-O-4 unit (A)
A_β(G)	83.79/4.39	C_β–H_β in β-O-4 linked to G (A)
B_α	85.44/4.67	C_α–H_α in resinol substructures (B)
A_β(S)	86.57/4.12	C_β–H_β in β-O-4 substructures linked to S units (A)
C_α	87.48/5.44	C_α–H_α in phenylcoumaran substructures (C)
$S_{2,6}$	104.49/6.71	$C_{2,6}$–$H_{2,6}$ in syringyl units (S)
$S'_{2,6}$	106.90/7.20	$C_{2,6}$–$H_{2,6}$ in oxidized syringyl units (S′)
G_2	111.56/6.99	C_2–H_2 in guaiacyl units (G)
G_5	115.57/6.80	C_5–H_5 in guaiacyl units (G)
G_6	119.64/6.79	C_6–H_6 in guaiacyl units (G)

The β-O-4, β-β, and β-5 are the main linkages of lignin, and their values can be calculated by a semi-quantitative 2D HSQC spectroscopy [48]. The results (per 100 Ar) were shown in Table 8. The relative content of β-O-4 in MWL and KL was 70.67/100Ar and 12.98/100Ar, respectively, which were attributed to a large number of β-O-4 aryl ethers that were depolymerized during the Kraft cooking process. In addition, the β-β linkages decreased from 14.38/100Ar to 7.14/100Ar and the signal of β-5 linkages was not detected. These were consistent with the weakening of β-O-4, β-β and β-5 signals in the NMR spectrum of KL. The S/G ratio in MWL and KL was 1.82 and 1.93, respectively. The results showed that the lignin macromolecules were depolymerized into micromolecules containing more S-type lignin during the Kraft cooking process [46].

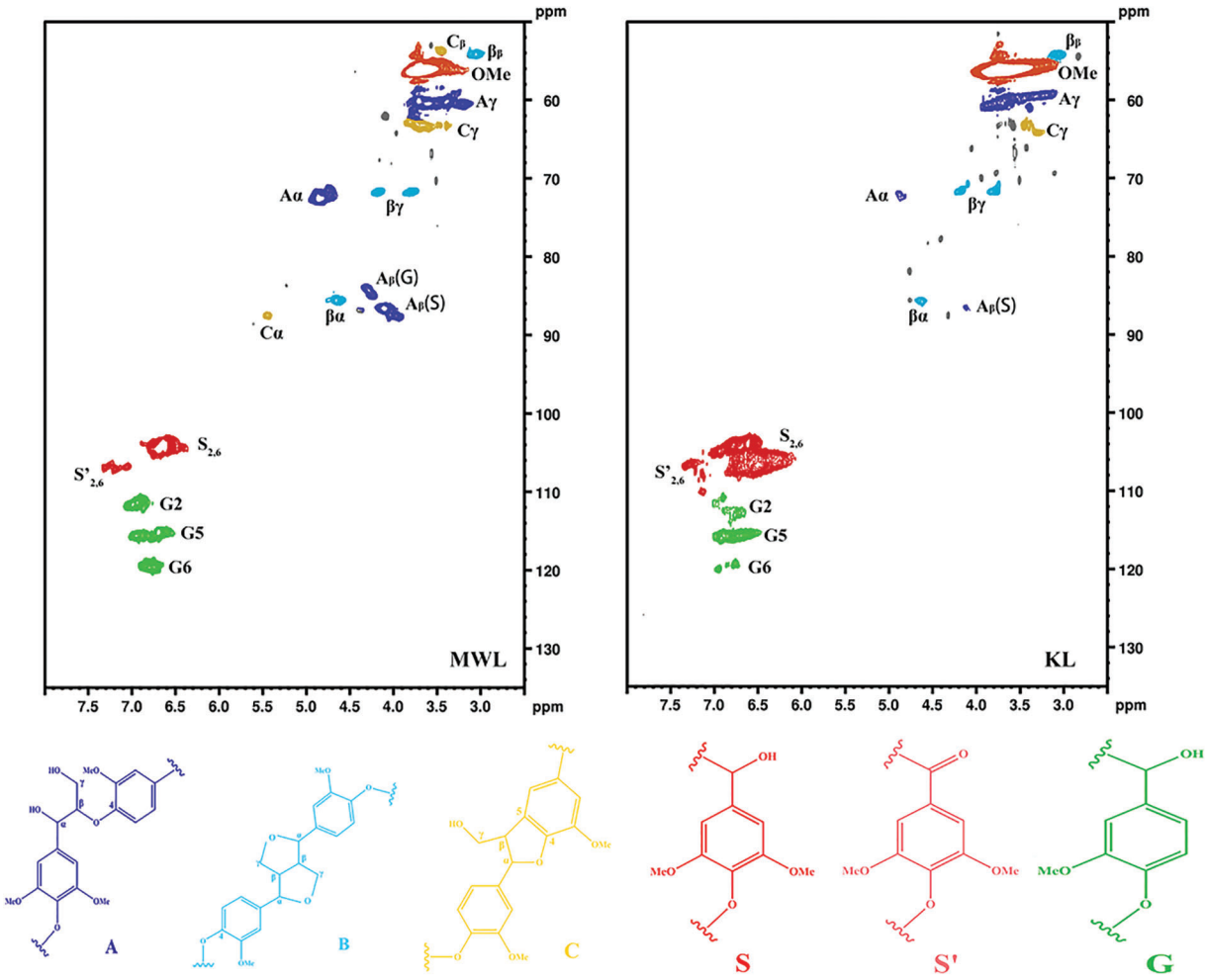

Figure 9: 2D-HSQC NMR spectra of MWL and KL

Table 8: Semi-quantitative 2D HSQC analysis of lignin substructures and linkages

Sample	β-O-4	β-β	β-5	S	G	S/G
MWL	70.67	14.38	1.50	64.54	35.46	1.82
KL	12.98	7.14	ND	65.84	34.16	1.93

Note: The values were presented on the basis of per 100 aromatic units; ND: Not detectable; S/G ratio = $0.5IS_{2,6}/IG_2$.

3.8.2 ^{31}P NMR analysis

The determination of hydroxyl content in lignin polymers is closely related to their further applications. The values of phenolic hydroxyl groups in lignin were determined by the quantitative ^{31}P NMR spectroscopy, and the results were shown in Table 9. As shown in Table 9, the content of A-OH groups in KL (0.50 mmol/g) was lower than that in MWL (3.80 mmol/g), which was attributed to the dehydration of the A-OH groups under the severe Kraft cooking conditions [47]. The content of total phenolic OH in KL (2.53 mmol/g) was higher than that in MWL (1.90 mmol/g), which was due to more phenolic OH groups were generated by cleaving the β-O-4 linkages in lignin [46]. This could be verified by β-O-4 linkages content in Table 8. Overall, the content of phenolic OH groups is a critical parameter reflecting the

antioxidant activity of lignin, so the high content of phenolic OH groups in KL can be applied in certain fields [49]. The content of the G-OH group (1.36 mmol/g) was higher than that of the S-OH group (0.37 mmol/g) in MWL, indicating that most of the syringyl groups in lignin existed as β-O-4 linkages [50]. In addition, the -COOH content (0.42 mmol/g) of KL was higher than MWL (0.32 mmol/g), indicating that part of the OH groups was oxidized to -COOH groups during the Kraft cooking process [46].

Table 9: Hydroxyl group contents of MWL and KL identified by quantitative ^{31}P NMR

Sample	Hydroxyl group content (mmol/g)					
	A-OH	S-OH	G-OH	CG-OH	Total phenolic hydroxyl	-COOH
MWL	3.80	0.37	1.36	0.17	1.90	0.32
KL	0.50	0.96	1.23	0.34	2.53	0.42

Note: A-OH: Aliphatic hydroxyl, S-OH: Syringyl phenolic hydroxyl, G-OH: Guaiacyl phenolic hydroxyl, CG-OH: Condensed guaiacyl phenolic hydroxyl.

3.9 Mass Balance of Converting Eucalyptus to Dissolving Pulp, Furfural and Kraft Lignin

A mass balance starting from 100 g (oven dry) of eucalyptus chips for our overall process was shown in Fig. 10. Based on this mass balance, 30.5 g dissolving pulp and 5.5 g furfural per 100 g eucalyptus chips (oven dry) were produced. Besides, 21.2 g Kraft lignin can be recovered, which will be a favorable feedstock for value-added products. It can be concluded that extremely low acid pretreatment exhibited great advantages throughout the overall process. The described parameters are of great significance for the industrial production of co-production of high-grade dissolving pulp, furfural, and Kraft lignin using eucalyptus.

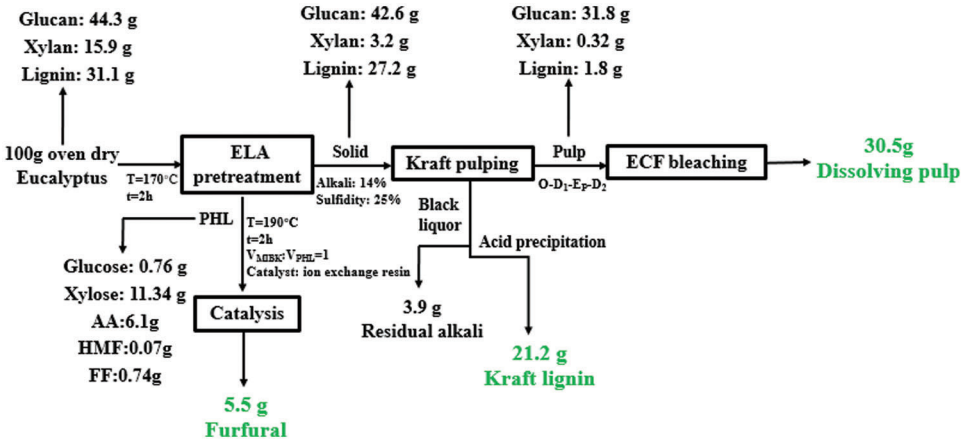

Figure 10: Mass balance for the overall process for the production of dissolving pulp, furfural, and Kraft lignin from eucalyptus

4 Conclusion

In the present study, co-production of high-grade dissolving pulp, furfural, and lignin from eucalyptus was established via these processes of extremely low acid pretreatment and Kraft pulping and ECF bleaching, catalytic conversion of xylose-rich pre-hydrolysate to furfural stages. Extremely low acid pretreatment can effectively remove 80.1% hemicellulose. Due to the removal of hemicellulose, the chemicals consumption in the subsequent cooking and bleaching stage was reduced. Compared with conventional hydrothermal pretreatment, the addition of extremely low acid can decrease the temperature of hydrothermal pretreatment by 10°C, which greatly reduces the energy consumption of enterprises.

High-grade dissolving pulp was obtained with an ISO brightness of 91.0%, viscosity of 618 mL/g, and α-cellulose content of 95.0%. 82.7% furfural yield and 82.9% furfural selectivity were obtained from xylose-rich pre-hydrolysate. The 2D-HSQC NMR and ^{31}P NMR analysis of Kraft lignin showed that β-O-4 aryl ethers were depolymerized in a large amount, and the S/G ratio and phenolic hydroxyl groups content increased during cooking during Kraft cooking process. Also, this new process of co-production of dissolving pulp, furfural, and lignin is suitable for biomass with high pentose content.

Funding Statement: This research was funded by the National Natural Science Foundation of China (No. 21978104) and the Program for the National Key Research and Development Program of China (No. 2021YFC2101601).

Conflicts of Interest: The authors declare that they have no conflicts of interest to report regarding the present study.

References

1. Ma, Y., Rosson, L., Wang, X., Byrne, N. (2019). Upcycling of waste textiles into regenerated cellulose fibres: Impact of pretreatments. *The Journal of the Textile Institute, 111(5),* 630–638. https://doi.org/10.1080/00405000.2019.1656355
2. Ütebay, B., Çelik, P., Çay, A. (2019). Effects of cotton textile waste properties on recycled fibre quality. *Journal of Cleaner Production, 222,* 29–35. https://doi.org/10.1016/j.jclepro.2019.03.033
3. Felgueiras, C., Azoia, N. G., Goncalves, C., Gama, M., Dourado, F. (2021). Trends on the cellulose-based textiles: Raw materials and technologies. *Frontiers in Bioengineering and Biotechnology, 9,* 608826. https://doi.org/10.3389/fbioe.2021.608826
4. Mendes, I. S. F., Prates, A., Evtuguin, D. V. (2021). Production of rayon fibres from cellulosic pulps: State of the art and current developments. *Carbohydrate Polymers, 273,* 118466. https://doi.org/10.1016/j.carbpol.2021.118466
5. Schier, F., Morland, C., Dieter, M., Weimar, H. (2021). Estimating supply and demand elasticities of dissolving pulp, lignocellulose-based chemical derivatives and textile fibres in an emerging forest-based bioeconomy. *Forest Policy and Economics, 126,* 102422. https://doi.org/10.1016/j.forpol.2021.102422
6. Arce, C., Llano, T., García, P., Coz, A. (2020). Technical and environmental improvement of the bleaching sequence of dissolving pulp for fibre production. *Cellulose, 27(7),* 4079–4090. https://doi.org/10.1007/s10570-020-03065-1
7. Kumar, H., Christopher, L. P. (2017). Recent trends and developments in dissolving pulp production and application. *Cellulose, 24(6),* 2347–2365. https://doi.org/10.1007/s10570-017-1285-y
8. Loureiro, P. E. G., Cadete, S. M. S., Tokin, R., Evtuguin, D. V., Lund, H. et al. (2021). Enzymatic fibre modification during production of dissolving wood pulp for regenerated cellulosic materials. *Frontiers in Plant Science, 12,* 717776. https://doi.org/10.3389/fpls.2021.717776
9. Yao, S., Nie, S., Yuan, Y., Wang, S., Qin, C. (2015). Efficient extraction of bagasse hemicelluloses and characterization of solid remainder. *Bioresource Technology, 185,* 21–27. https://doi.org/10.1016/j.biortech.2015.02.052
10. Kaur, I., Ni, Y. (2015). A process to produce furfural and acetic acid from pre-hydrolysis liquor of kraft based dissolving pulp process. *Separation and Purification Technology, 146,* 121–126. https://doi.org/10.1016/j.seppur.2015.03.034
11. Luo, Y., Li, Z., Li, X., Liu, X., Fan, J. et al. (2019). The production of furfural directly from hemicellulose in lignocellulosic biomass: A review. *Catalysis Today, 319,* 14–24. https://doi.org/10.1016/j.cattod.2018.06.042
12. Ajao, O., Marinova, M., Savadogo, O., Paris, J. (2018). Hemicellulose based integrated forest biorefineries: Implementation strategies. *Industrial Crops and Products, 126,* 250–260. https://doi.org/10.1016/j.indcrop.2018.10.025
13. Demuner, I. F., Colodette, J. L., Demuner, A. J., Jardim, C. M. (2019). Biorefinery review: Wide-reaching products through kraft lignin. *BioResources, 14(3),* 7543–7581. https://doi.org/10.15376/biores

14. Dessbesell, L., Paleologou, M., Leitch, M., Pulkki, R., Xu, C. (2020). Global lignin supply overview and kraft lignin potential as an alternative for petroleum-based polymers. *Renewable and Sustainable Energy Reviews, 123,* 109768. https://doi.org/10.1016/j.rser.2020.109768
15. Kim, J. S., Lee, Y. Y., Torget, R. W. (2001). Cellulose hydrolysis under extremely low sulfuric acid and high-temperature conditions. *Applied Biochemistry and Biotechnology, 91(1),* 331–340.
16. Gurgel, L. V. A., Marabezi, K., Ramos, L. A., Curvelo, A. A. D. S. (2012). Characterization of depolymerized residues from extremely low acid hydrolysis (ELA) of sugarcane bagasse cellulose: Effects of degree of polymerization, crystallinity and crystallite size on thermal decomposition. *Industrial Crops and Products, 36(1),* 560–571. https://doi.org/10.1016/j.indcrop.2011.11.009
17. Lee, J. Y., Kim, Y. S., Um, B. H., Oh, K. (2013). Pretreatment of laminaria japonica for bioethanol production with extremely low acid concentration. *Renewable Energy, 54,* 196–200. https://doi.org/10.1016/j.renene.2012.08.025
18. Lee, J., Li, P., Lee, J., Ryu, H. J., Oh, K. K. et al. (2013). Ethanol production from saccharina japonica using an optimized extremely low acid pretreatment followed by simultaneous saccharification and fermentation. *Bioresource Technology, 127,* 119–25. https://doi.org/10.1016/j.biortech.2012.09.122
19. Hu, B., Cheng, A. S., Xie, W. L., Liu, J., Huang, Y. B. et al. (2022). The oxalic acid-assisted fast pyrolysis of biomass for the sustainable production of furfural. *Fuel, 322,* 124279. https://doi.org/10.1016/j.fuel.2022.124279
20. Song, L., Wang, R., Jiang, J., Xu, J., Gou, J. (2020). Stepwise separation of poplar wood in oxalic acid/water and gamma-valerolactone/water systems. *RSC Advances, 10(19),* 11188–11199. https://doi.org/10.1039/D0RA01163K
21. Penin, L., Lopez, M., Santos, V., Alonso, J. L., Parajo, J. C. (2020). Technologies for eucalyptus wood processing in the scope of biorefineries: A comprehensive review. *Bioresource Technology, 311,* 123528. https://doi.org/10.1016/j.biortech.2020.123528
22. Sun, S., Cao, X., Li, H., Chen, X., Tang, J. et al. (2018). Preparation of furfural from eucalyptus by the MIBK/H_2O pretreatment with biphasic system and enzymatic hydrolysis of the resulting solid fraction. *Energy Conversion and Management, 173,* 539–544. https://doi.org/10.1016/j.enconman.2018.08.006
23. Sluiter, A., Hames, B., Ruiz, R. O., Scarlata, C., Sluiter, J. et al. (2008). Determination of structural carbohydrates and lignin in biomass. *Laboratory Analytical Procedure, 1617(1),* 1–16.
24. BjÖRkman, A. (1954). Isolation of lignin from finely divided wood with neutral solvents. *Nature, 174(4440),* 1057–1058. https://doi.org/10.1038/1741057a0
25. Wang, X., Li, H., Lin, Q., Li, R., Li, W. et al. (2019). Efficient catalytic conversion of dilute-oxalic acid pretreated bagasse hydrolysate to furfural using recyclable ironic phosphates catalysts. *Bioresource Technology, 290,* 121764. https://doi.org/10.1016/j.biortech.2019.121764
26. Li, H., Ren, J., Zhong, L., Sun, R., Liang, L. (2015). Production of furfural from xylose, water-insoluble hemicelluloses and water-soluble fraction of corncob via a tin-loaded montmorillonite solid acid catalyst. *Bioresource Technology, 176,* 242–248. https://doi.org/10.1016/j.biortech.2014.11.044
27. Segal, L., Creely, J. J., Martin, A. E., Conrad, C. M. (1959). An empirical method for estimating the degree of crystallinity of native cellulose using the X-ray diffractometer. *Textile Research Journal, 29(10),* 786–794. https://doi.org/10.1177/004051755902901003
28. Tizazu, B. Z., Moholkar, V. S. (2018). Kinetic and thermodynamic analysis of dilute acid hydrolysis of sugarcane bagasse. *Bioresource Technology, 250,* 197–203. https://doi.org/10.1016/j.biortech.2017.11.032
29. Hu, F., Ragauskas, A. (2014). Suppression of pseudo-lignin formation under dilute acid pretreatment conditions. *RSC Advances, 4(9),* 4317–4323. https://doi.org/10.1039/C3RA42841A
30. Li, S. X., Li, M. F., Bian, J., Sun, S. N., Peng, F. et al. (2017). Biphasic 2-methyltetrahydrofuran/oxalic acid/water pretreatment to enhance cellulose enzymatic hydrolysis and lignin valorization. *Bioresource Technology, 243,* 1105–1111. https://doi.org/10.1016/j.biortech.2017.07.075
31. Springer, E. L., Harris, J. F. (1985). Procedures for determining the neutralizing capacity of wood during hydrolysis with mineral acid solutions. *Industrial & Engineering Chemistry Product Research and Development, 24,* 485–489. https://doi.org/10.1021/i300019a030

32. Lin, L., Ma, X. J., Cao, S. L., Luo, X. L., Chen, L. H. et al. (2014). Relationship of pH of the hydrolysate and the yield of bamboo in oxalic acid treatment. *Transactions of China Pulp and Paper, 29,* 11–15.
33. Deng, A., Ren, J., Li, H., Peng, F., Sun, R. (2015). Corncob lignocellulose for the production of furfural by hydrothermal pretreatment and heterogeneous catalytic process. *RSC Advances, 5(74),* 60264–60272. https://doi.org/10.1039/C5RA10472F
34. Zhang, T., Li, W., An, S., Huang, F., Li, X. (2018). Efficient transformation of corn stover to furfural using p-hydroxybenzenesulfonic acid-formaldehyde resin solid acid. *Bioresource Technology, 264,* 261–267. https://doi.org/10.1016/j.biortech.2018.05.081
35. Chen, Y., Yan, Z., Liang, L., Ran, M., Wu, T. et al. (2020). Comparative evaluation of organic acid pretreatment of eucalyptus for kraft dissolving pulp production. *Materials, 13(2),* 361. https://doi.org/10.3390/ma13020361
36. Tyufekchiev, M., Kolodziejczak, A., Duan, P., Foston, M., Schmidt-Rohr, K. et al. (2019). Reaction engineering implications of cellulose crystallinity and water-promoted recrystallization. *Green Chemistry, 21(20),* 5541–5555. https://doi.org/10.1039/C9GC02466B
37. Donohoe, B. S., Decker, S. R., Tucker, M. P., Himmel, M. E., Vinzant, T. B. (2008). Visualizing lignin coalescence and migration through maize cell walls following thermochemical pretreatment. *Biotechnology and Bioengineering, 101(5),* 913–925. https://doi.org/10.1002/bit.21959
38. Xiao, L. P., Sun, Z. J., Shi, Z. J., Xu, F., Sun, R. C. (2011). Impact of hot compressed water pretreatment on the structural changes of woody biomass for bioethanol production. *BioResources, 6(2),* 1576–1598.
39. Mendes, C. V. T., Carvalho, M. G. V. S., Baptista, C. M. S. G., Rocha, J. M. S., Soares, B. I. G. et al. (2009). Valorisation of hardwood hemicelluloses in the kraft pulping process by using an integrated biorefinery concept. *Food and Bioproducts Processing, 87(3),* 197–207. https://doi.org/10.1016/j.fbp.2009.06.004
40. Dong, Y., Ji, H., Dong, C., Zhu, W., Long, Z. et al. (2020). Preparation of high-grade dissolving pulp from *radiata* pine. *Industrial Crops and Products, 143,* 111880. https://doi.org/10.1016/j.indcrop.2019.111880
41. Shafiei, M., Latibari, A. J. (2015). Alkaline-sulfite/Anthraquinone (As/Aq) pulping of old corrugated container and elemental chlorine free (ECF) bleaching of the pulp. *Cellulose Chemistry and Technology, 49(9–10),* 841–846.
42. Andrade, M. F., Colodette, J. L. (2014). Dissolving pulp production from sugar cane bagasse. *Industrial Crops and Products, 52,* 58–64. https://doi.org/10.1016/j.indcrop.2013.09.041
43. Lee, C. B. T. L., Wu, T. Y. (2021). A review on solvent systems for furfural production from lignocellulosic biomass. *Renewable and Sustainable Energy Reviews, 137,* 110172. https://doi.org/10.1016/j.rser.2020.110172
44. Lin, Q., Zhan, Q., Li, R., Liao, S., Ren, J. et al. (2021). Solvent effect on xylose-to-furfural reaction in biphasic systems: Combined experiments with theoretical calculations. *Green Chemistry, 23(21),* 8510–8518. https://doi.org/10.1039/D1GC02812J
45. Davaritouchaee, M., Hiscox, W. C., Terrell, E., Mancini, R. J., Chen, S. (2020). Mechanistic studies of milled and kraft lignin oxidation by radical species. *Green Chemistry, 22(4),* 1182–1197. https://doi.org/10.1039/C9GC04162A
46. Wei, X., Liu, Y., Luo, Y., Shen, Z., Wang, S. et al. (2021). Effect of organosolv extraction on the structure and antioxidant activity of eucalyptus kraft lignin. *International Journal of Biological Macromolecules, 187,* 462–470. https://doi.org/10.1016/j.ijbiomac.2021.07.082
47. Sun, S. C., Sun, D., Li, H. Y., Cao, X. F., Sun, S. N. et al. (2021). Revealing the topochemical and structural changes of poplar lignin during a two-step hydrothermal pretreatment combined with alkali extraction. *Industrial Crops and Products, 168,* 113588. https://doi.org/10.1016/j.indcrop.2021.113588
48. Chen, W. J., Zhao, B. C., Cao, X. F., Yuan, T. Q., Shi, Q. et al. (2019). Structural features of alkaline dioxane lignin and residual lignin from eucalyptus grandis x E. urophylla. *Journal of Agricultural and Food Chemistry, 67(3),* 968–974. https://doi.org/10.1021/acs.jafc.8b05760
49. Espinoza-Acosta, J. L., Torres-Chávez, P. I., Ramírez-Wong, B., López-Saiz, C. M., Montaño-Leyva, B. (2016). Antioxidant, antimicrobial, and antimutagenic properties of technical lignins and their applications. *BioResources, 11(2),* 5452–5481. https://doi.org/10.15376/biores
50. Wang, H. M., Wang, B., Wen, J. L., Yuan, T. Q., Sun, R. C. (2017). Structural characteristics of lignin macromolecules from different eucalyptus species. *ACS Sustainable Chemistry & Engineering, 5(12),* 11618–11627. https://doi.org/10.1021/acssuschemeng.7b02970